Physica B 674 (2024) 415594

Contents lists available at ScienceDirect

Physica B: Condensed Matter

journal homepage: www.elsevier.com/locate/physb

# Coupling-induced bistability in self-oscillating regimes of two coupled identical Spin-Torque Nano-oscillators

S. Perna [a,*], M. Anand [a], G. Oliviero [a], A. Quercia [a], M. d'Aquino [a], S. Wittrock [b], R. Lebrun [c], V. Cros [c], C. Serpico [a]

[a] Università di Napoli Federico II, Dipartimento di Ingegneria Elettrica e Tecnologie dell'Informazione, Via Claudio 21, Napoli, 80125, Italy
[b] Helmholtz-Zentrum Berlin fur Materialien und Energie GmbH, Hahn-Meitner-Platz 1, Berlin, 14109, Germany
[c] Unité Mixte de Physique CNRS, Thales, Université Paris-Saclay, 1 Avenue Augustin Fresnel, 91767, Palaiseau, France

ARTICLE INFO

*Keywords:*
Spin-torque nano-oscillators
Magnetization dynamics
Stuart–Landau oscillators

ABSTRACT

We consider a system of two coupled identical Spin Torque Nano-Oscillators (STNOs) with cylindrical geometry. The STNOs have free layers in the vortex magnetization configuration and fixed layer with magnetization in the out-of-plane direction. The magnetization dynamics in the two STNOs are analyzed by using a Thiele-like equation governing the dynamics of the vortex core positions. The coupling is assumed to be linear and symmetric and this enables to characterize it by a single complex parameter. We consider numerical simulations of the model as a function of the coupling strength $k$ and phase $\phi_k$. Depending on their values, different motions of the vortex cores are observed, e.g. periodic, and quasi-periodic. Each type of dynamics can be classified according to the symmetry property shown by the trajectories. In this respect, the transition between different types of motion corresponds to a symmetry-breaking process and we describe it as a bifurcation process. Fixing the value of the coupling constant phase, we found that there is a range of coupling constant strength in which the periodic and quasi-periodic motions coexist and both are stable. This bistability is an interesting phenomenon in connection to research on neuromorphic circuits based on STNOs.

## 1. Introduction

Spin-Torque Nano-Oscillators (STNOs) are promising candidates for the design and the realization of electric current tunable oscillators suitable for various applications in Information and Communication Technologies [1]. A central topic in this area is studying and controlling the dynamics of two or more coupled STNOs. Considerable research has been carried out in the analysis of synchronization of STNOs as this phenomenon is instrumental for increasing the oscillators emitted power [2–5]. More recently, increasing attention has been paid to the study of coupled STNOs in connection with spintronic-based neuromorphic computations [6–8].

In this work, we consider the dynamics of two identical cylindrical STNOs, with the free layer in the vortex state [9], that are linearly and symmetrically coupled. The magnetization oscillations in the STNOs are a consequence of the dynamics of the two vortex cores that are excited by the currents injected in the oscillators. The geometries and the excitation conditions of the STNOs are such that each of them is rotationally symmetric. In this situation, the physical system has two symmetries: it is invariant under the exchange of the oscillators and with respect to simultaneous and equal rotations of both oscillators with respect to the respective axes of symmetry. The breaking of these symmetries has an important role in the qualitative dynamics of the system and leads to the presence of coexisting stable steady oscillatory states. In this respect, by using a combination of analytical and numerical results, we explore how, in the presence of coexisting stable regimes, a particular steady state can be reached by changing the strength of the coupling between STNOs. This possibility of controlling coupled oscillator dynamics by changing the coupling strength is relevant to neuromorphic computation where coupling strength plays the role of an artificial synaptic weight [6,8].

From the modeling point of view, magnetization vortex evolutions in the free layers of the STNOs are described by the method of collective variables [10,11]. This leads to coupled Thiele-like equations [12] governing the evolution of the position of the vortex cores [13–15]. Considering the rotational symmetry of each STNO and by using appropriate normalizations, the equations describing the coupled dynamics of the vortex cores can be rewritten as the equations of two identical coupled Stuart-Landau oscillators [16]. The Stuart-Landau oscillator (SLO) is a canonical model to study self-oscillations and the dynamics

* Corresponding author.
*E-mail address:* salvatore.perna@unina.it (S. Perna).

https://doi.org/10.1016/j.physb.2023.415594
Received 31 July 2023; Received in revised form 1 December 2023; Accepted 9 December 2023
Available online 14 December 2023

of two coupled SLOs is the standard model to study mutual synchronization of two oscillators. More specifically, we consider the case of linear and symmetric coupling which can be justified on the basis of general theoretical considerations [17], for moderately small deviations of the vortex core from the rest position. In this context, the coupling is controlled by a single complex-valued parameter. The limit of weak coupling (small coupling coefficient) can be studied by assuming constant oscillation amplitudes with the model of phase oscillators [16]. This model enables to study mutual synchronization [18]. When the coupling strength is increased the dynamics of the oscillators have to be analyzed by taking into account also the oscillation amplitudes evolution [15,19]. In this case, the dynamics is richer and novel phenomena arise in the bifurcation patterns of the dynamical system. In this respect, it has been recently studied the solutions of coupled SLOs exhibit exchange symmetry breaking while keeping the rotational symmetry of the solution [20]. This phenomenon along with the possible symmetry breakings of the rotational symmetry of the solution is central in this study. The guiding idea is to use the breaking of symmetries to identify and control coexisting steady states as a function of the coupling strength.

## 2. Mathematical model

We consider a system of two interacting and identical STNOs driven by injected electric currents as sketched in Fig. 1. The interaction of the two STNOs can be realized by means of different physical mechanisms such as direct electrical connections, electromagnetic fields generated by the STNOs, or systems of antennas inductively coupled with the oscillators [21]. In the present work, however, this aspect is not crucial as the described phenomenon does not depend on the specific physical nature of the coupling. Regarding the physical structure of STNOs, these are multilayered cylindrical structures that include ferromagnetic 'fixed layer' and 'free layer', separated by a nonmagnetic spacer. The fixed layer, with constant magnetization, acts as a spin polarizer for the injected electric current. Both the fixed layer magnetization and the direction of current flow are parallel to the axis of the cylindrical structure (out-of-plane direction). The free layer is where magnetization changes under the influence of external excitations and the magnetization dynamics is governed by the Landau-Lifshitz-Gilbert-Sloncewski equation governing the dynamics of magnetization in the free layers:

$$\frac{d\boldsymbol{m}}{dt} - \alpha \boldsymbol{m} \times \frac{d\boldsymbol{m}}{dt} = -\boldsymbol{m} \times \boldsymbol{h}_{\text{eff}} + \boldsymbol{\tau}_{\text{ST}}\,, \tag{1}$$

where $\boldsymbol{m}$ is the free layer magnetization unit-vector, $t$ is time expressed in units of $(\gamma M_s)^{-1}$ ($\gamma = 2.21\times10^5$ s$^{-1}$ A$^{-1}$ m is the absolute value of the gyromagnetic ratio and $M_s$ is the free layer saturation magnetization), $\alpha$ is the Gilbert damping. The effective field $\boldsymbol{h}_{\text{eff}} = -\delta g/\delta \boldsymbol{m}$ is the variational derivative of the micromagnetic free energy $g[\boldsymbol{m}]$ given by

$$g[\boldsymbol{m}] = \frac{1}{V}\int_V \left[\frac{l_{\text{ex}}^2}{2}(\nabla \boldsymbol{m})^2 - \frac{\boldsymbol{h}_m \cdot \boldsymbol{m}}{2} - \boldsymbol{h}_a \cdot \boldsymbol{m}\right] dV\,, \tag{2}$$

where $V$ is the free layer volume, $l_{\text{ex}} = \sqrt{2A/(\mu_0 M_s^2)}$ is the exchange length of the material ($A$ is the exchange constant), $\boldsymbol{h}_m$ is the magnetostatic field, $\boldsymbol{h}_{\text{a}}$ is the field due to the injected currents and to sources external to the free layer under examination. The last term in Eq. (1) is given by $\boldsymbol{\tau}_{\text{ST}} = \beta \boldsymbol{m} \times (\boldsymbol{m} \times \boldsymbol{e}_z)$ is the spin-torque term, where $\boldsymbol{e}_z$ is the unit vector in the out-of-plane direction. The parameter $\beta$ plays the role of normalized injected current density such that $\beta = \sigma J/M_s$, $\sigma = \hbar P/(2\mu_0|e|LM_s)$ is the spin-torque efficiency ($\hbar$ is the Planck constant, $P$ is the polarization factor, $\mu_0$ is the vacuum permeability, $e$ is the electron charge) and $L$ is the thickness of the free layer. Field-like spin torque is neglected. The geometry of the system is such that magnetization in the free layer is in magnetic vortex state, and gyration of vortex core around its rest position (fundamental mode) are driven by the spin-torque effect associated with the spin-polarized injected currents.

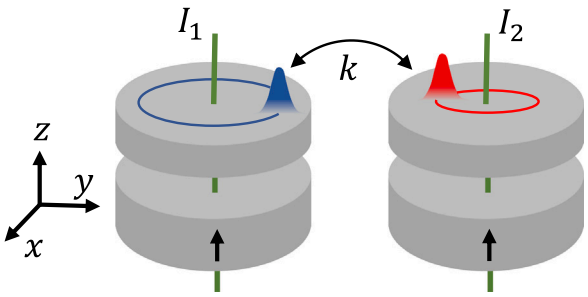


**Fig. 1.** Sketch of coupled Spin-Torque Nano-Oscillators (STVOs). The upper layers are the free layers of the STNOs with magnetization in vortex state (bell-shaped symbols) and the lower layers are the fixed layer of the STNOs with magnetization (black arrows) pointing along the $z$-direction. The parameter $k$ represents the strength of the coupling.

Vortex dynamics is described by a Thiele-like equation governing the dynamics of the vortex-core positions in the two STNOs.

The Thiele-like equation is obtained from Eq. (1) by introducing, as a set of collective variables, the vortex core positions in the free layers [10], and by considering the appropriate vortex ansatz [22] $\boldsymbol{m}_k(\boldsymbol{\rho}_k, t) = \boldsymbol{m}_V(\boldsymbol{\rho}_k, \mathbf{x}_k(t))$, with $k = 1, 2$, for the free layer of both oscillators, where $\boldsymbol{\rho}_k$ is the in-plane position vectors and $\mathbf{x}_k$ are vortex core displacements from the center of the free layers measured in units of the radius $R$ of the STNOs. This leads to the following equation governing the evolution of the vortex cores dynamics [12,14] :

$$\boldsymbol{e}_z \times \frac{d\mathbf{x}_k}{dt} + \omega \mathbf{x}_k + a\frac{d\mathbf{x}_k}{dt} + \beta c \boldsymbol{e}_z \times \mathbf{x}_k + \boldsymbol{f}_{\text{C}}\,. \tag{3}$$

In Eq. (3), $\omega(\text{x}, \beta)$ is the natural frequency of the conservative vortex oscillations associated with the free energy of the vortex $w(\text{x}, \beta)$ as follows [23]:

$$\omega(\text{x}, \beta) = \frac{1}{\text{x}}\frac{dw}{d\text{x}}(\text{x}, \beta)\,. \tag{4}$$

The third and fourth term in Eq. (3), are respectively associated to damping and spin-torque effects. In this respect, $a(\text{x}, \beta)$ is the damping constant and $c$ is a parameter which can be estimated by the formula $c = \pi/(Sg_0)$ where $g_0 = 2\pi p/S$ is the so-called gyrofactor, $p$ is the vortex polarity, and $S = \pi R^2$ is the free layer cross-section. The fourth term in Eq. (3), $\boldsymbol{f}_{\text{C}}(\mathbf{x}_1, \mathbf{x}_2)$ is the term describing the coupling of the two STNOs. The specific form of this term depends on the nature of the coupling.

By vector multiplying both sides of Eq. (3) by $\boldsymbol{e}_z$ and using the fact that the quantity $a$, $\beta$ and $\boldsymbol{f}_{\text{C}}$ are small quantities with respect to $\omega$, Eq. (3), can be transformed in the following form

$$\frac{d\mathbf{x}_k}{dt} = \omega(\text{x}_k, \beta)\boldsymbol{e}_z \times \mathbf{x}_k - a(\text{x}_k, \beta)\omega \mathbf{x}_k + \beta c \mathbf{x}_k + \boldsymbol{b}_{C,k}(\mathbf{x}_1, \mathbf{x}_2)\,, \tag{5}$$

where $\boldsymbol{b}_{C,k}(\mathbf{x}_1, \mathbf{x}_2) = -\boldsymbol{e}_z \times \boldsymbol{f}_{\text{C}}(\mathbf{x}_1, \mathbf{x}_2)$. In the case when the vortex displacement $\mathbf{x}_1$, $\mathbf{x}_2$ are small enough, and under the assumption of symmetric coupling, on the basis of general considerations about coupled systems [17], it is possible to consider that the coupling function has the following linear form:

$$\boldsymbol{b}_{C,1} = K \cdot (\mathbf{x}_2 - \mathbf{x}_1)\,, \tag{6}$$

$$\boldsymbol{b}_{C,2} = K \cdot (\mathbf{x}_1 - \mathbf{x}_2)\,, \tag{7}$$

where $K$ is a $2 \times 2$ matrix given by the following expression

$$K = \begin{bmatrix} k_d & -k_c \\ k_c & k_d \end{bmatrix} \tag{8}$$

By making use of the natural association of two-dimensional vectors $\mathbf{x}_k$ with complex number $z_k$, the coupled Eqs. (9), can be written as

$$\begin{aligned} \frac{dz_1}{dt} &= (\lambda + j\omega_0 + \gamma|z_1|^2)z_1 + ke^{j\phi_k}(z_2 - z_1) \\ \frac{dz_2}{dt} &= (\lambda + j\omega_0 + \gamma|z_2|^2)z_2 + ke^{j\phi_k}(z_1 - z_2)\,, \end{aligned} \tag{9}$$

where $\lambda = \beta c - a\omega_0$, $\omega_0 = \omega(\mathbf{0}, \beta)$, $\gamma = -a\omega_1 + j\omega_1$, with $\omega_1$ the coefficient weighting the nonlinear shift of the frequency with the vortex displacement, namely $\omega = \omega_0 + \omega_1|z|^2$, $k = \sqrt{k_c^2 + k_d^2}$, and $\phi_k = \arctan(k_c/k_d)$.

We remark, that although Eq. (9) has been derived considering the coupled dynamics of two magnetic vortices, its range of applications can be extended to several types of coupled oscillators [24], as well as the conclusions we derive from it in the following sections.

## 3. Classification of the oscillating solutions

The system of equations so obtained has been investigated in the literature [17,19–21,24]. Its structural properties come directly from the symmetries of the physical system that it models. In particular, it remains unchanged under the reflection transformation, namely $(z_1, z_2) \to (z_2, z_1)$. This means that, given a solution $(z_1(t), z_2(t))$, we can get another solution under the same transformation. Such property is a direct consequence of the invariance of the physical system when the two STNOs are exchanged. The other property is the invariance of the equations under equal rotation of both complex variables in the respective complex planes, namely $z_i \to e^{j\theta} z_i$ where $\theta$ is the rotation angle and $i = 1, 2$. This property is a consequence of the fact that the physical system does not change under equal rotation of both STNOs around the $z$-axis.

The system of Eq. (9) has two invariant manifolds. The first is the two-dimensional subspace of $(z_1, z_2)$, which is four-dimensional, such that $z_1 = z_2$. The dynamics of the coupled oscillator system for initial conditions $z_1(0) = z_2(0)$ is described by the following Stuart-Landau (SL) equation:

$$\frac{dz}{dt} = (\lambda + j\omega_0 + \gamma|z|^2)z\,. \tag{10}$$

The solution to this SL equation is called the symmetric solution and can be expressed in analytical form [25]. The SL equation is also known as Hopf bifurcation normal-form [26] since it shows a Hopf bifurcation at the equilibrium $z = 0$ when $\lambda = 0$. Steady and stable self-oscillations with radius $r = |z| = \sqrt{-\lambda/\gamma_r}$ are observed for $\lambda > 0$ and $\gamma_r = \Re[\gamma] < 0$, where $\Re[.]$ is the real part operator. This stability property has to be referred to perturbations on the manifold $z_1 = z_2$. In general, the conditions $\lambda > 0$ and $\gamma_r < 0$ do not guarantee the stability for the symmetric self-oscillations. The symmetric self-oscillation remains unchanged under equal rotation in the complex plane of both complex variables. For this, they are said to be $S^1$-symmetric. They also have the exchange symmetry property, namely they remain unchanged by the reflection transformation. In the following, this self-oscillation will be termed $S^1$-S P-mode.

The other invariant manifold is the two-dimensional subspace of the space $(z_1, z_2)$ such that $z_1 = -z_2$. The dynamics of the coupled oscillator system for initial conditions $z_1(0) = -z_2(0)$ is described by a SL equation (see Eq. (10)) with the following parameters: $\lambda \to \tilde{\lambda} = \lambda - 2k\cos\phi_k$ and $\omega_0 \to \tilde{\omega}_0 = \omega_0 - 2k\sin\phi_k$. Self-oscillations on this manifold are said to be antisymmetric. Notice that the existence of stable antisymmetric self-oscillations on the manifold $z_1 = -z_2$ is connected to values of coupling strength and phase. Antisymmetric self-oscillations are $S^1$-symmetric and they have broken exchange symmetry. This means that if you apply the reflection transformation to one antisymmetric oscillation state, the result is new antisymmetric oscillation. A further application of the reflection transformation brings the oscillatory state to the initial one. This self-oscillation will be termed $S^1$-BA P-mode.

In addition to symmetric and antisymmetric self-oscillations, Eq. (9) admits a third class of self-oscillations with $S^1$-symmetry that has a more general form of broken exchange symmetry: $z_1(t) = \sigma z_2(t)$, where the constant $\sigma = |\sigma|\, e^{j\phi_\sigma} \in \mathbb{C}$. Like antisymmetric self-oscillations, this kind of self-oscillations can only exist in pairs. This self-oscillation will be termed $S^1$-B P-mode.

In our numerical investigations, which will be discussed in detail in the next section, we observe a fourth type of solution that is with broken $S^1$-symmetry and with broken exchange symmetry. This type of solution corresponds to a quasi-periodic oscillatory state. This type of oscillation will be termed Q-mode.

In the following, we characterize the transitions between different types of oscillations as a consequence of a bifurcation process. In this respect, let us write the system of Eq. (9) in polar coordinates $(\rho_1, \rho_2, \phi_1, \phi_2)$ as in the following:

$$\begin{aligned}
\dot{\rho}_1 &= (\hat{\lambda} + \gamma_r\rho_1^2)\rho_1 + k\rho_2\cos(\phi_k + \phi)\,,\\
\dot{\rho}_2 &= (\hat{\lambda} + \gamma_r\rho_2^2)\rho_2 + k\rho_1\cos(\phi_k - \phi)\,,\\
\dot{\phi}_1 &= (\hat{\omega}_0 + \gamma_i\rho_1^2) + k\frac{\rho_2}{\rho_1}\sin(\phi_k + \phi)\,,\\
\dot{\phi}_2 &= (\hat{\omega}_0 + \gamma_i\rho_2^2) + k\frac{\rho_1}{\rho_2}\sin(\phi_k - \phi)\,,
\end{aligned} \tag{11}$$

where $\hat{\lambda} = \lambda - k\cos\phi_k$, $\hat{\omega}_0 = \omega_0 - k\sin\phi_k$ and $\phi = \phi_2 - \phi_1$. In this form, we recognize that the independent dynamic variables are three, namely $\rho_1$, $\rho_2$, $\phi$. This fact is expected due to the invariance of Eq. (9) when the complex variable $z_1$, $z_2$ are rotated by equal angle in the respective complex planes. The equation governing the dynamics of $\phi$ can be easily obtained by taking the difference between the fourth and third equations. In this way, we get the following equation:

$$\dot{\phi} = \gamma_i(\rho_2^2 - \rho_1^2) + k\left(\frac{\rho_1}{\rho_2}\sin(\phi_k - \phi) - \frac{\rho_2}{\rho_1}\sin(\phi_k + \phi)\right)\,. \tag{12}$$

The set of equations made by the first two of Eqs. (11) and (12) is particularly convenient because P-modes correspond to equilibria $\dot{\rho}_1 = \dot{\rho}_2 = \dot{\phi} = 0$. Therefore the study of the bifurcations involving P-modes can be reduced to a local bifurcation analysis. The linearized equations of motion in the space $(\rho_1, \rho_2, \phi)$, that will be used for local bifurcations analysis, are given by the following ones:

$$\begin{aligned}
\delta\dot{\rho}_1 =& (\hat{\lambda} + 3\gamma_r\rho_1^2)\,\delta\rho_1 + k\cos(\phi + \phi_k)\,\delta\rho_2\\
&- k\rho_2\sin(\phi + \phi_k)\,\delta\phi\,,\\
\delta\dot{\rho}_2 =& k\cos(\phi_k - \phi)\,\delta\rho_1 + (\hat{\lambda} + 3\gamma_r\rho_2^2)\,\delta\rho_2\\
&+ k\,\rho_1\sin(\phi_k - \phi)\,\delta\phi\,,\\
\delta\dot{\phi} =& \Omega_{\rho_1}\delta\rho_1 + \Omega_{\rho_2}\delta\rho_2 + \Omega_\phi\delta\phi\,,
\end{aligned} \tag{13}$$

where

$$\begin{aligned}
\Omega_{\rho_1} =& k\rho_2\left(\frac{1}{\rho_2^2}\sin(\phi_k - \phi) + \frac{1}{\rho_1^2}\sin(\phi_k + \phi)\right)\\
&- 2\gamma_i\rho_1\,,\\
\Omega_{\rho_2} =& -k\rho_1\left(\frac{1}{\rho_2^2}\sin(\phi_k - \phi) + \frac{1}{\rho_1^2}\sin(\phi_k + \phi)\right)\\
&+ 2\gamma_i\rho_2\,,\\
\Omega_\phi =& -k\left(\frac{\rho_1}{\rho_2}\cos(\phi_k - \phi) + \frac{\rho_2}{\rho_1}\cos(\phi_k + \phi)\right)\,.
\end{aligned} \tag{14}$$

The set of Eq. (13) are in the form $\delta\dot{\boldsymbol{x}} = \boldsymbol{J}(\boldsymbol{x})\cdot\delta\boldsymbol{x}$, where $\boldsymbol{x} = (\rho_1, \rho_2, \phi)$, and $\dot{\boldsymbol{x}} = \mathbf{0}$. The local bifurcation analysis is based on the variation as a function of the coupling strength of the eigenvalues of the Jacobian matrix $\boldsymbol{J}(\boldsymbol{x})$.

In the next section, the bifurcation mechanisms responsible for the transition between the presented oscillatory dynamics will be investigated numerically and with analytical techniques according to the approach presented in this section.

## 4. Results

The two STNOs considered have the following physical and geometrical parameters: radius $R = 100\,\text{nm}$, thickness $L = 5\,\text{nm}$, saturation magnetization $M_s = 800\,\text{kA/m}$, gyromagnetic ratio $g_r = 28\,\text{GHz/T}$, exchange stiffness $l_{\text{ex}} = 5.7\,\text{nm}$ and Gilbert damping $\alpha = 0.02$. From these parameters, the following ones correspond in Eq. (9) [27]: $\omega_0 = 0.0177$, which in dimensional units corresponds to about $2\pi 250\,\text{MHz}$, $\omega_1 = 0.25\,\omega_0$, and $a = 0.0246$. The features of the two linearly coupled

vortices nonlinear dynamics have been investigated by numerical integration of Eq. (9) with varying $k$. In particular, we did a numerical analysis where we changed it quasi-statically and kept its phase fixed. In this context, quasi-static means that for each value of the coupling strength the dynamic is integrated for a large enough time interval to assume that a steady oscillatory regime, even in the presence of non-periodic oscillations (Q-mode), is reached. From the dynamics at regime the maxima of $|z_1|$ and $|z_2|$ are recorded. We refer to these quantities in the figures shown in the following as extreme of $|z|$. The final condition of a simulation is used as the initial condition for the next simulation where the coupling strength has a different value. Fig. 2 shows the extreme of $|z|$ as a function of $k$. Depending on the value of $k$ different types of oscillations are observed. The following fixed parameters are used: $\lambda = 0.15\,a\,\omega_0$, and $\phi_k = 0.4\,\pi$. In the figure, each branch of the diagram corresponds to an icon whose meaning is indicated in Fig. 3. For $k = 0$, the two SL equations are uncoupled and then they have the same dynamics but with an arbitrary phase difference which is set by the initial condition. The regime self-oscillation is an $S^1$-B P-mode when the initial phases of the two complex variables are different. In this respect, an $S^1$-S P-mode is observed when the initial phases are the same. For $0 < k < k_t$ two $S^1$-BA P-modes are observed. One can be obtained by reflection from the other. Therefore, $k = 0$ corresponds to a pitchfork bifurcation. This can be verified from Eq. (13) by observing that the determinant of the Jacobian matrix vanishes, which is due to the fact that one of the eigenvalues is equal to zero. Moreover, for a very small value of the coupling strength we expect that self-oscillations are characterized by $\rho_1 = \rho_2$ which from Eq. (11) is possible when $\phi = \pi$. In the presence of $S^1$-BA P-modes, we have steady oscillations with $|z_1| = |z_2| = |z| = \sqrt{-(\lambda - 2k\cos\phi_k)/\gamma_r}$. This explains why in Fig. 2 the extreme of $|z|$ decreases when $k$ is increased. For $k_t < k < k_c$ simulations show a stable Q-mode. The transition $S^1$-BA P-mode $\rightarrow$ Q-mode occurs for $k = k_t$, that corresponds to a Neimark-Sacker or torus bifurcation [26]. The value of $k_t$ can be found by setting to zero the real part of the eigenvalue of $\boldsymbol{J}(z_1 = -z_2)$. This derivation can be found in Ref. [20], and it permits to arrive to the following relation:

$$k_t = \frac{\lambda}{4\cos\phi_k}\,. \tag{15}$$

In the range $k_t < k \leq k_c$ the dynamic of the coupled oscillators in terms of the polar coordinates covers a torus manifold. This is because such an oscillation mode has frequency components which in general have not a rational ratio (see Fig. 6). The time necessary to cover the torus manifold is theoretically infinite but if the integration time is large enough, the covering becomes almost complete. As already mentioned the Q-mode neither possesses $S^1$-symmetry nor exchange symmetry. However, once the torus is covered, if we project the solution onto the respective complex planes corresponding to the two STNOs, we discover that these symmetries are recovered. This is a very interesting topic, but a deeper discussion on it is out of the scope of this work. For $k = k_c$ the Q-mode approaches to the $S^1$-S P-mode. After that, an $S^1$-B P-mode is observed. In the following, we give more details about this transition, but before that, we focus on what happens when $k$ is further increased. The $S^1$-B P-modes remain stable for $k_c < k < k_p$. For $k = k_p$ they merge into the symmetric one stabilizing it. For $0 < k < k_p$ the $S^1$-S P-mode is stable only against perturbations occurring on the invariant manifold $z_1 = z_2$. In this respect, in the three-dimensional space $(\rho_1, \rho_2, \phi)$ this oscillation corresponds to a saddle equilibrium point. For $k > k_p$ the $S^1$-S P-mode becomes stable against any perturbation in the four-dimensional space. Therefore, $k = k_p$ corresponds to a pitchfork bifurcation, where the value of $k_p$ can be found by setting to zero the real part of the eigenvalue of $\boldsymbol{J}(z_1 = z_2)$. Such derivation is given in Ref. [20] and it produces the following relation:

$$k_p = -\lambda(\cos\phi_k + (\gamma_i/\gamma_r)\sin\phi_k)\,. \tag{16}$$

If $k$ is decreased from a value $k > k_p$, the dynamics will occur on the invariant manifold $z_1 = z_2$ even for values $k < k_p$. The coexistence of

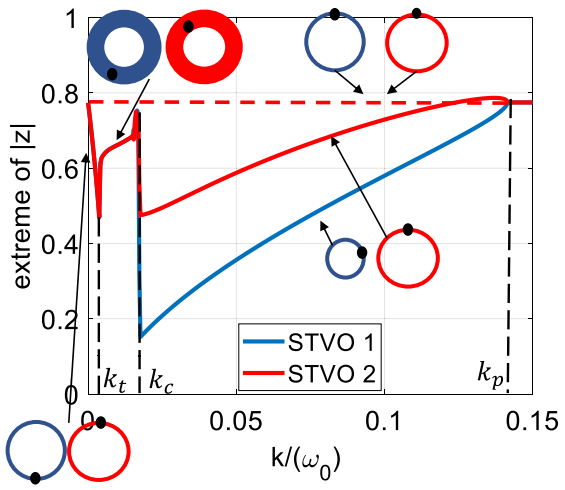


**Fig. 2.** Extreme of $|z|$ as a function of the coupling strength $k$. The symbols on the figure are specified in the table in Fig. 3. Continuous lines indicate that the respective oscillation is stable while a dashed line indicates that it is unstable. The vertical black dashed lines specify the value of $k$ where a transition between two different types of oscillation is observed.

| Icon | Name | $S_1$ | Exch. | $\phi$ | $\rho_1/\rho_2$ |
|---|---|---|---|---|---|
| | $S^1$-S P-mode | Yes | Yes | 0 | 1 |
| | $S^1$-BA P-mode | Yes | No | $\pi$ | 1 |
| | $S^1$-B P-mode | Yes | No | $\phi_\sigma$ | $\lvert\sigma\rvert$ |
| | Q-mode | No | No | f.o.t | f.o.t |

**Fig. 3.** Legend for the symbols used to identify the several oscillations observed in numerical simulations. The distinction is made on the basis of $S^1$-symmetry, exchange symmetry, phase $\phi$ and ratio of the orbit radius for the two STNOs. The acronym f.o.t stays for function of time.

different (in terms of symmetry properties) stable oscillatory regimes is found by repeating the same kind of simulations where $k$ is first increased and then decreased in a range such that $\max k < k_p$. Therefore, the initial condition used for the first simulation of the sequence at decreasing $k$ has to be a $S^1$-B P-mode. In this way, we discover that for $k_h < k < k_c$ there is the coexistence of stable $S^1$-B P-modes and the Q-mode. When $k$ is decreased starting from a $S^1$-B P-mode, the transition to the Q-mode occurs at a value $k = k_h < k_c$. This coexistence produces the hysteresis loop shown in Fig. 4, which has not been investigated elsewhere.

Let us discuss in more detail the transitions observed for $k = k_c$ and for $k = k_h$. In the first case, when $k$ takes values close to $k_c$, the time evolution of the amplitudes $|z_1|$, $|z_2|$ is similar to that shown in Fig. 5. We also observe from numerical simulations that as $k$ approaches $k_c$ the sensitivity to initial conditions increases. By analyzing in the frequency domain this phenomenon, we see that for $k_t < k < k_c$ the spectrum of $z_i(t)$ is multi peaked, and as $k$ approaches $k_c$ it becomes continuous. This is shown in Fig. 6. Then, when for $k > k_c$ the oscillations become $S^1$-B P-mode, and as a consequence of that the spectrum becomes single peaked. A fine scanning in a range of $k$ very close to $k_c$ reveals that for $k = k_c$ there is a contact between the Q-mode and the $S^1$-S P-mode.

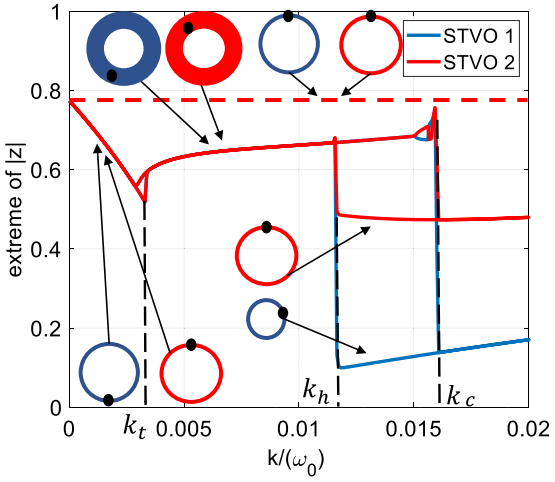


**Fig. 4.** Extreme of $|z|$ as a function of the coupling strength $k$. The symbols on the figure are specified in the table in Fig. 3. Continuous lines indicate that the respective oscillation is stable while a dashed line indicates that it is unstable. The vertical black dashed lines specify the value of $k$ where a transition between two different types of oscillation is observed.

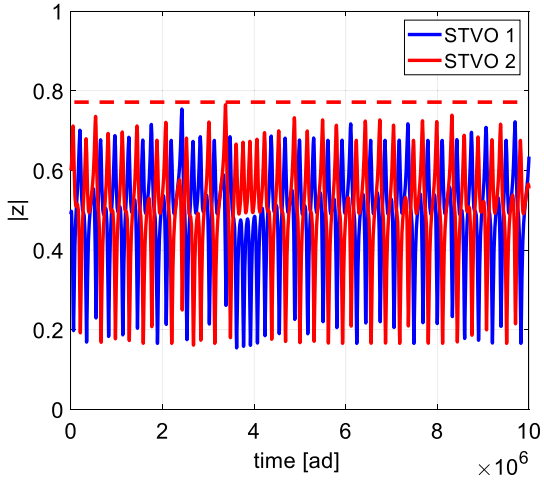


**Fig. 5.** Time evolution of $|z(t)|$ for both STNOs for $\phi_k = 0.4\pi$ and $k$ very close to $k_c$ from the left. The dashed lines indicate the symmetric oscillation.

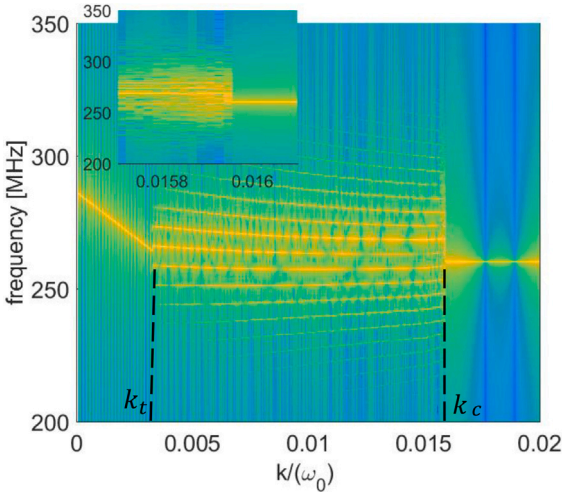


**Fig. 6.** Spectrum of $z_1(t)$ as a function of the coupling constant. The same spectrum is obtained by considering $z_2(t)$. The vertical black dashed lines specify the value of $k$ where a transition between two different types of oscillation is observed. The spectrum is plotted on a logarithmic scale.

In the three-dimensional space $(\rho_1, \rho_2, \phi)$ this process corresponds to a limit cycle, corresponding to the Q-mode, that breaks on a saddle point corresponding to the $S^1$-S P-mode. The bifurcation mechanism responsible for the inverse transition occurring at $k = k_h$ is different from the one just discussed. In order to investigate it, we first compute the $S^1$-B P-mode as a solution of the system of equations $\dot{\boldsymbol{x}} = \boldsymbol{0}$, where $\boldsymbol{x} = (\rho_1, \rho_2, \phi)$. This calculation is made by programming a suitable Newton–Raphson routine (NR) starting from a non-symmetric initial solution, namely $(\rho_1, \phi_1) \neq (\rho_2, \phi_2)$. In this process, the numerical continuation method is used, namely the final solution of the NR corresponding to a certain value of $k$ is used as the initial solution for the next calculation where the coupling strength has a different value. The consistency of our calculations is shown in Fig. 7 where the extreme of $|z|$ obtained from numerical time integration and those corresponding to $S^1$-symmetric self-oscillations computed with the NR are compared. Once the point in the $(\rho_1, \rho_2, \phi)$ space corresponding to the $S^1$-B P-mode is determined, we use it to compute the eigenvalues of the Jacobian matrix when $k$ is decreased. In this way, we find out that among the three eigenvalues, one of them is real and negative and the real parts of two of them for $k > k_h$ are negative, vanish at $k = k_h$, and for lower values of $k$ become positive. This bifurcation process corresponds to a subcritical Neimark-Sacker bifurcation [26]. The set of bifurcation, when the coupling strength is changed, is now complete. The next question is what happens to this picture when the phase of the coupling is changed. In Fig. 8 the phase diagram of the bifurcations in the plane $(\phi_k, k)$ is shown. For values of the coupling constant phase $\phi_k > 0.17\pi$, the sequence of bifurcations observed by changing $k$ is the same as for the case $\phi_k = 0.4\pi$ previously discussed. The range of coupling strength values in which there is a stable Q-mode, for a fixed value of the coupling phase $\phi_k$, can be estimated by taking the difference $k_c(\phi_k) - k_t(\phi_k)$. On the other hand, the range of coupling strength values in which there is a stable $S^1$-B P-mode, for a fixed value of the coupling phase, can be estimated by taking the difference $k_p(\phi_k) - k_h(\phi_k)$. Therefore, the range of coupling strength values in which there is the coexistence of these two types of oscillations can be estimated by taking the difference $k_c(\phi_k) - k_h(\phi_k)$. New bifurcation curves for values of the coupling constant phase $\phi_k \leq 0.17\pi$ emerge. They are plotted in the figure in light green and blue. These curves are obtained by analyzing the zero crossing of the real part of the eigenvalues of $S_1$-B P-mode when the coupling constant strength is changed. They correspond to sub-critical Neimark-Sacker bifurcations. In the presence of these bifurcations, the range of coupling strength values in which the coexistence between $S^1$-B P-modes and the Q-mode changes. If we imagine repeating the numerical experiment where the coupling strength is first increased up to a value smaller than $k_p(\phi_k)$ and then decreased, such coexistence range is squeezed to zero if the green curve intercepts the curve $k = k_h(\phi_k)$ (yellow curve in the figure). This aspect is still under investigation and will be discussed in more details in a future publication.

## 5. Conclusion

In this work, the nonlinear dynamics of two linearly coupled with free layers in the vortex state have been investigated when the coupling between the oscillators is changed. Several regimes of oscillations are observed and they have been classified according to the symmetry properties that they possess. The transitions between different types of oscillations have been explained in terms of bifurcation processes. By using combined analytical and numerical techniques we are able to draw the phase diagram in the plane $(\phi_k, k)$, where the region where several types of oscillations can be observed. We found that for a fixed value of coupling constant phase, there exists a range of coupling constant strength values in which there is bistability of different types

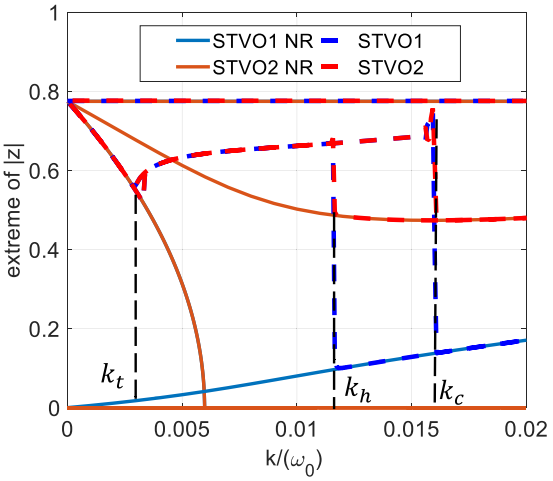


**Fig. 7.** Extreme of $|z|$ as a function of the coupling strength $k$. Continuous lines indicate the $S^1$-symmetric self-oscillations computed with the Newton–Raphson routine, while the dashed lines indicate the oscillations computed by numeric integration of Eq. (9). The vertical black dashed lines specify the value of $k$ where a transition between two different types of oscillation is observed.

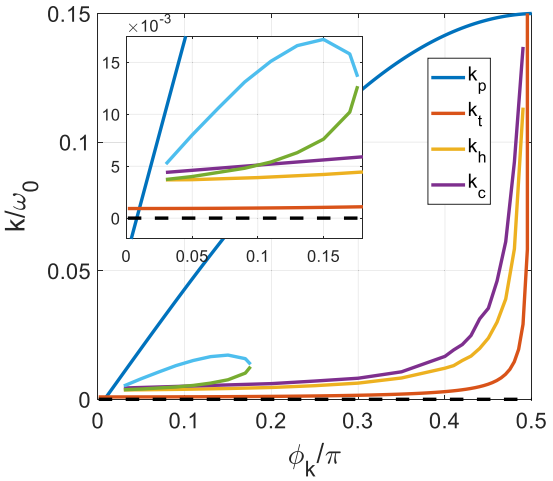


**Fig. 8.** Phase diagram of the dynamical system (9) in the plane $(\phi_k, k)$. The inset indicates two additional Neimark-Sacker bifurcations occurring on the $S^1$-B P-modes.

of oscillations and therefore there is a hysteretic relation between the type of oscillation observed and the value of the coupling constant strength, and this range changes as the phase changes. For small values of the coupling constant phase, there are bifurcation processes that first reduce and then annihilate the range of coupling constant strength where there is coexistence.

In conclusion, we believe that this study represents a step toward a deeper comprehension of the nonlinear dynamics of coupled STNOs. As we have shown, the role of the coupling between oscillators is crucial. Indeed, for a fixed device, a proper coupling value allows observing several different and eventually coexisting oscillatory regimes. This can be of utmost importance for microwave technology and neuromorphic computing systems based on STNO technology. On the other hand, our study will be of help to scholars for future investigations where the number of coupled devices is larger than two or where nonlinear models of coupling are used.

## CRediT authorship contribution statement

**S. Perna:** Formal analysis, Investigation, Methodology, Validation, Writing – original draft, Writing – review & editing. **M. Anand:** Visualization, Writing – review & editing. **G. Oliviero:** Writing – review & editing. **A. Quercia:** Investigation, Writing – review & editing. **M. d'Aquino:** Supervision, Writing – review & editing, Methodology. **S. Wittrock:** Investigation, Writing – review & editing. **R. Lebrun:** Investigation, Writing – review & editing. **V. Cros:** Methodology, Supervision, Writing – review & editing. **C. Serpico:** Conceptualization, Investigation, Methodology, Supervision, Writing – original draft, Writing – review & editing.

## Declaration of competing interest

The authors declare that they have no known competing financial interests or personal relationships that could have appeared to influence the work reported in this paper.

## Data availability

All data supporting the findings of this study are available within the article and, they are available from the corresponding author on reasonable request.

## Acknowledgment

The authors acknowledge financial support from the Horizon 2020 Framework Programme of the European Commission under FET-Open grant agreement no. 899646 (k-NET).

## References

[1] B. Dieny, et al., Opportunities and challenges for spintronics in the microelectronics industry, Nat. Electron. 3 (2020) 446–459.
[2] R. Lebrun, S. Tsunegi, P. Bortolotti, H. Kubota, A.S. Jenkins, M. Romera, K. Yakushiji, A. Fukushima, J. Grollier, S. Yuasa, V. Cros, Mutual synchronization of spin torque nano-oscillators through a long range and tunable electrical coupling scheme, Nature Commun. 8 (2017) 15825.
[3] M. Zahedinejad, A.A. Awad, S. Muralidhar, et al., Two-dimensional mutually synchronized spin hall nano-oscillator arrays for neuromorphic computing, Nat. Nanotechnol. 15 (2020) 47–52.
[4] A. Quercia, M. d'Aquino, V. Scalera, S. Perna, C. Serpico, Normal form of nonlinear oscillator model relevant to spin-torque nano-oscillator theory, Physica B 549 (2018).
[5] T. Chen, et al., Spin-torque and spin-hall nano-oscillators, Proc. IEEE 104 (10) (2016) 1919–1945.
[6] J. Torrejon, M. Riou, F.A. Araujo, S. Tsunegi, G. Khalsa, D. Querlioz, P. Bortolotti, V. Cros, K. Yakushiji, A. Fukushima, H. Kubota, S. Yuasa, M.D. Stiles, J. Grollier, Neuromorphic computing with nanoscale spintronic oscillators, Nature 547 (2017) 428.
[7] Hanuman Singh, et al., Mutual synchronization of spin-torque nano-oscillators via oersted magnetic fields created by waveguides, Phys. Rev. Appl. 11 (2019) 054028.
[8] J. Grollier, D. Querlioz, K.Y. Camsari, et al., Neuromorphic spintronics, Nat. Electron 3 (2020) 360–370.
[9] A. Dussaux, B. Georges, J. Grollier, V. Cros, A.V. Khvalkovskiy, A. Fukushima, M. Konoto, H. Kubota, K. Yakushiji, S. Yuasa, K.A. Zvezdin, K. Ando, A. Fert, Large microwave generation from current-driven magnetic vortex oscillators in magnetic tunnel junctions, Nat. Commun. 1 (2010) 8.
[10] O.A. Tretiakov, D. Clarke, Gia-Wei Chern, Ya.B. Bazaliy, O. Tchernyshyov, Dynamics of domain walls in magnetic nanostrips phys, Rev. Lett. 100 (2008) 127204.
[11] D.J. Clarke, O.A. Tretiakov, G.-W. Chern, Ya.B. Bazaliy, O. Tchernyshyov, Dynamics of a vortex domain wall in a magnetic nanostrip: Application of the collective-coordinate approach, Phys. Rev. B 78 (2010) 134412.
[12] A.A. Thiele, Steady-state motion of magnetic domains, Phys. Rev. Lett. 30 (1973) 230.
[13] K.Y. Guslienko, R.H. Heredero, O. Chubykalo-Fesenko, Phys. Rev. B 82 (2010) 014402.
[14] K.Y. Guslienko, O.V. Sukhostavets, D.V. Berkov, Nonlinear magnetic vortex dynamics in a circular nanodot excited by spin-polarized current, Nanoscale Res. Lett. 9 (2014) 386.

[15] M. d'Aquino, S. Perna, A. Quercia, V. Scalera, C. Serpico, Current-driven hysteretic synchronization in vortex nanopillar spin-transfer oscillators, IEEE Magn. Lett. 8 (2017) 3504005.
[16] Y. Kuramoto, Chemical Oscillations, Waves, and Turbulence, Springer, 2012.
[17] D.G. Aronson, E.J. Doedel, H.G. Othmer, An analytical and numerical study of the bifurcations in a system of linearly-coupled oscillators, Physica D 25 (1987) 20–104.
[18] A. Balanov, N. Janson, D. Postnov, O. Sosnovtseva, Synchronization, from Simple To Complex, Springer, 2009.
[19] D.G. Aronson, G.B. Ermentrout, N. Kopell, Amplitude response of coupled oscillators, Physica D 41 (1990) 403–449.
[20] A. Röhm, K. Lüdge, I. Schneider, Bistability in two simple symmetrically coupled oscillators with symmetry-broken amplitude- and phase-locking, Chaos 28 (2018) 063114.
[21] S. Wittrock, et al., Non-hermiticity in spintronics: oscillation death in coupled spintronic nano-oscillators through emerging exceptional points, arXiv:2108.04804v2.
[22] K.Yu. Guslienko, K.L. Metlov, Evolution and stability of a magnetic vortex in a small cylindrical ferromagnetic particle under applied field, Phys. Rev. B 63 (2001) 100403.
[23] K.Yu. Guslienko, B.A. Ivanov, V. Novosad, Y. Otani, H. Shima, K, Fukamichi; eigenfrequencies of vortex state excitations in magnetic submicron-size disks, J. Appl. Phys. 91 (10) (2002) 8037–8039.
[24] A. Slavin, V. Tiberkevich, Nonlinear auto-oscillator theory of microwave generation by spin-polarized current, IEEE Trans. Magn. 45 (4) (2009) 1875–1918.
[25] J. Stuart, On the non-linear mechanics of hydrodynamic stability, J. Fluid Mech. 4 (1) (1958) 1–21.
[26] Y.A. Kutnezov, Elements of Applied Bifurcation Theory, third ed., Springer Verlag, New York, 2004.
[27] P. Bortolotti, et al., Parametric excitation of magnetic vortex gyrations in spin-torque nano-oscillators, Phys. Rev. B 88 (2013) 174417.